Journal of the Optical Society of Korea
Vol. 20, No. 5, October 2016, pp. 614-622

ISSN: 1226-4776(Print) / ISSN: 2093-6885(Online)
DOI: http://dx.doi.org/10.3807/JOSK.2016.20.5.614

Design Method for a Total Internal Reflection LED Lens with Double Freeform Surfaces for Narrow and Uniform Illumination

Jae Suk Yang, Jae-Hyeung Park, Beom-Hoan O, Se-Geun Park, and Seung Gol Lee*

School of Information & Communication Engineering, Inha University, Inha-ro 100, Inchon, 22212, Korea

(Received June 14, 2016 : revised August 22, 2016 : accepted September 2, 2016)

In this paper, we propose a novel differential equation method for designing a total internal reflection (TIR) LED lens with double freeform surfaces. A complete set of simultaneous differential equations for the method is derived from the condition for minimizing the Fresnel loss, illumination models, Snell's Law of ray propagation, and a new constraint on the incident angle of a ray on the light-exiting surface of the lens. The last constraint is essential to complete the set of simultaneous differential equations. By adopting the TIR structure and applying the condition for minimizing the Fresnel loss, it is expected that the proposed TIR LED lens can have a high luminous flux efficiency, even though its beam-spread angle is narrow. To validate the proposed method, three TIR LED lenses with beam-spread angles of less than 22.6° have been designed, and their performances evaluated by ray tracing. Their luminous flux efficiencies could be obviously increased by at least 35% and 5%, compared to conventional LED lenses with a single freeform surface and with double freeform surfaces, respectively.

Keywords : Double freeform surfaces, TIR LED lens, Luminous flux efficiency, Fresnel loss, Narrow beam-spread angle
OCIS codes : (220.2740) Geometric optical design; (220.2945) Illumination design; (080.4298) Nonimaging optics; (080.4225) Nonspherical lens design; (230.3670) Light-emitting diodes

I. INTRODUCTION

Compared to conventional light sources such as incandescent and fluorescent lamps, light emitting diodes (LEDs) are safe sources that have advantages, such as higher efficiency, longer lifetime, and more environmentally friendly aspects [1]. Thanks to such advantages, LEDs are widely used in various kinds of indoor and outdoor lighting, indicator lights, and display devices [2-6]. However, since the luminous flux emitted from an LED has a Lambertian distribution, secondary optics for controlling the luminous flux are necessary to form a desired illuminance distribution on a target plane [7]. The secondary optics can be implemented as a reflective optical system, a refractive optical system, or a hybrid optical system in which reflective and refractive systems are combined. A refractive optical system is preferred, for the sake of lumiaire compactness. The secondary optics based on a refractive optical system are simply called an "LED lens".

The LED lens can be designed using a differential equation method [8-11], a parameter optimization method [12-15], or a simultaneous multiple surface (SMS) method [16-18], and it often includes one or more freeform surfaces, for the sake of low price and high efficiency. The differential equation method is an LED lens design method in which differential equations relating to the propagation of rays through an LED lens are solved assuming that one surface of the lens is already known; then the other surface is freeform. In this method, first the location of a ray of light emitted from the LED to impinge on a target plane is determined, depending on an illumination model selected to form a desired illuminance distribution on the target plane. Then the surface slope of a corresponding incident point on the freeform surface is determined so that the ray incident upon the surface will pass through a designated point on the target plane [8-11]. Though the freeform surface is easily determined, as long as the related simultaneous differential equations can be derived completely, the luminous

*Corresponding author: sglee@inha.ac.kr

This is an Open Access article distributed under the terms of the Creative Commons Attribution Non-Commercial License (http://creativecommons.org/licenses/by-nc/3.0/) which permits unrestricted non-commercial use, distribution, and reproduction in any medium, provided the original work is properly cited.

Copyright © 2016 Optical Society of Korea

flux efficiency of an LED lens with a single freeform free-form surface is limited by the other surface that is *not* set as the freeform surface. Parameter optimization is another design method, in which all surfaces of an LED lens are described parametrically, and the parameter values are adjusted using an optimization method so that a desired illuminance distribution can be formed, and simultaneously the maximum luminous flux efficiency can be attained [12-15]. However, the parameter optimization method has a drawback, in that the lens performance depends on the initial values of the parameters and may become trapped in a local minimum during optimization. In particular, the method entails a problem in that the number of the parameters increases with increasing complexity of the shape of an LED lens, thus making optimization difficult. Finally, in the SMS method, since all surfaces of an LED lens must be controlled to obtain the desired performance, much time is inevitably required to calculate a large amount of information about the lens surface [16-18].

Since an LED lens with a single freeform surface has a limitation in controlling the luminous flux emitted from an LED, as mentioned previously, design methods for an LED lens with double freeform surfaces (double freeform-surface lens) have received much attention recently [19-24]. Unfortunately, geometric optics cannot provide the necessary and sufficient conditions for making the simultaneous differential equations for a double freeform-surface lens complete, contrary to the case of a single freeform surface [19, 25]. In other words, double freeform surfaces cannot be determined uniquely without introducing additional constraints. Various additional constraints have been introduced to resolve this problem. For instance, a condition for minimizing the Fresnel loss was used as an additional constraint in reference [19]. This refers to the condition that the deflection angle of a ray on a light-entering surface of an LED lens must be identical to that on a light-exiting surface of the same lens, to minimize the total reflection loss approximately. In reference [20] a more rigorous condition for minimizing the sum of two Fresnel losses occurring at both the light-entering surface and light-exiting surface of the lens was used. In addition, different design methods for a double freeform-surface lens suffer from similar incompleteness. The combination of the edge-ray and luminance-engineering principles was used to resolve the problem in reference [22], and the so-called integrability condition for the surface normal vectors was used in reference [23]. A double freeform-surface lens for shaping a laser beam has been designed using two conditions on the intensity and phase distributions [24].

Usually, a double freeform-surface lens is superior in luminous flux efficiency to an LED lens with a single freeform surface. For example, a double freeform-surface lens shown at the reference [19] can have a higher luminous flux efficiency, even at a beam-spread angle of less than 100^{o}, compared to a conventional LED lens with a single freeform surface. However, if the required beam-spread angle is less than 40^{o}, the luminous flux efficiency cannot be improved any more, despite the application of the condition for minimizing the Fresnel loss [19]: Because a ray that is incident upon the peripheral region of the lens must be deflected strongly to make its beam-spread angle narrow, reflection loss occurring at the peripheral region of the lens is not reduced, thus making it impossible to improve the luminous flux efficiency.

In this paper we propose a new differential equation method for designing a total internal reflection (TIR) LED lens with double freeform surfaces, in which a TIR structure is adopted to reduce deflection angles on both the light-entering surface and the light-exiting surface. Compared to a conventional LED lens without a TIR surface, a TIR LED lens has a relatively small deflection angle on the light-entering and light-exiting surfaces [26]. Accordingly, it is expected to reduce reflection loss further by applying the condition for minimizing Fresnel loss simultaneously, although the beam-spread angle is narrow. In a TIR LED lens, the central refraction part is composed of a light-entering surface and a light-exiting surface, as in a conventional LED lens, and thus two surfaces can be designed as freeform surfaces according to the method described in the reference [19]. However, the peripheral TIR part of the TIR LED lens includes a light-entering surface, a light-exiting surface, and a TIR surface, and thus a new differential equation method for determining the three freeform surfaces is required. We have derived the simultaneous differential equations required for the proposed method, where an additional constraint is introduced to form a complete set, so that all surfaces of the peripheral TIR part can be designed as freeform surfaces.

In Section II, we establish a differential equation method for the peripheral TIR part of the TIR LED lens, and describe a process for introducing the additional constraint needed for the design. In Section III, we introduce the design procedure for the TIR LED lens. In Section IV, we describe design results according to the proposed method, and the improvement in luminous flux efficiency. Finally, we present the conclusion of this paper.

II. DIFFERENTIAL EQUATION METHOD FOR A TIR LED LENS WITH DOUBLE FREEFORM SURFACES

Let us examine the shape of the TIR LED lens and the propagation of rays through the lens as shown in Fig. 1, to derive a complete set of simultaneous differential equations for the proposed method. The lens, shown in an *x*-*z* Cartesian coordinate system, includes a central refraction part and a peripheral TIR part, and has rotational symmetry with respect to the *z* axis. Hereafter the refractive index of the lens is referred to as *n*. The central refraction part is composed of an inner surface (corresponding to a light-entering surface) including a point $\mathbf{P}_{1a}$, and an outer surface (corresponding to a light-exiting surface) including a point $\mathbf{P}_{1c}$. The peripheral TIR part is composed of a side surface (corresponding to

a light-entering surface) including a point $\mathbf{P}_{2a}$, a TIR surface including a point $\mathbf{P}_{2b}$, an outer surface (corresponding to a light-exiting surface) including a point $\mathbf{P}_{2c}$, and a bottom surface that connects the side surface and TIR surface. The bottom surface does not act on the propagation of the light ray. The inner surface of the central refraction part and the side surface of the peripheral TIR part intersect at point $\mathbf{C}_{IS}$, and the outer surfaces of the central refraction part and the peripheral TIR part intersect at point $\mathbf{C}_{OO}$. In addition, the outer surface and the TIR surface of the peripheral TIR part intersect at point $\mathbf{C}_{OT}$, and the end points of the bottom surface are referred to as $\mathbf{C}_{SB}$ and $\mathbf{C}_{BT}$ respectively.

In Fig. 1, the distance between a light source **S** positioned at the origin of the coordinate system and an incident point on either the inner surface or the side surface is defined as R, and the emission angle φ of light emitted from the light source is defined with respect to the z axis. The emission angle of light incident upon the intersection point $\mathbf{C}_{IS}$ is referred to as the split angle φ_{split}. It is assumed that rays passing through the central refraction part reach the entire region of a target plane according to a divergent illumination model, and that rays passing through the peripheral TIR part reach the target plane according to a convergent illumination model [27].

Ray ①, which is a representative ray of light passing through the central refraction part, is emitted from **S** and is incident upon the point $\mathbf{P}_{1a}$ on the inner surface. The ray refracted at the point $\mathbf{P}_{1a}$ is incident upon the point $\mathbf{P}_{1c}$ on the outer surface, and the distance between points $\mathbf{P}_{1a}$ and $\mathbf{P}_{1c}$ is l_{ac}. The ray finally reaches a point $\mathbf{P}_{1T}$ on the target plane, and the x-axis distance between the central axis of the target plane and $\mathbf{P}_{1T}$ is ρ. In the central refraction part, the propagation angles of the ray refracted on the inner and outer surfaces are γ and β, and are defined as the angles formed by the z axis and the rays. The propagation angle of the ray that is rotated clockwise with respect to the z axis is defined as having a positive value. Since the rays passing through the central refraction part follow a divergent illumination model, the propagation angles γ and β always have positive values, irrespective of the emission angle φ.

Meanwhile, ray ②, which is a representative ray of light passing through the peripheral TIR part, is emitted from **S** and is incident upon the point $\mathbf{P}_{2a}$ on the side surface. The ray finally reaches a point $\mathbf{P}_{2T}$ on the target plane after passing through a point $\mathbf{P}_{2b}$ on the TIR surface and a point $\mathbf{P}_{2c}$ on the outer surface. The distances between $\mathbf{P}_{2a}$ and $\mathbf{P}_{2b}$ and $\mathbf{P}_{2b}$ and $\mathbf{P}_{2c}$ are referred to as l_{ab} and l_{bc} respectively. In addition, the propagation angles of the rays refracted on the side surface, incident upon the outer surface, and refracted on the outer surface are α, δ, and β respectively. The propagation angles δ and β are defined with respect to the z axis, but exceptionally the propagation angle α, measured counterclockwise with respect to the x axis, is defined as having a positive value. Since the rays passing through the peripheral TIR part follow a convergent illumination model, a ray whose emission angle φ is slightly larger than φ_{split} must reach the peripheral region of the target plane, and a ray whose emission angle φ is maximum ($\varphi = \varphi_{max}$) must reach the center of the target plane. Thus the signs of the propagation angles δ and β may vary, depending on the emission angle of the ray at the peripheral TIR part. Ray ② is a ray whose propagation angles δ and β have positive values, while ray ③'s propagation angles have negative values.

The central refraction part of the lens is determined by three unknown functions, R, γ, and l_{ac}, and the peripheral TIR part of the lens is determined by five unknown functions, R, α, l_{ab}, l_{bc}, and β. All unknown functions determining the surfaces of a lens are functions of an emission angle φ. The relationship (complete set of simultaneous differential equations) between the three unknown functions relevant to the central refraction part has been already described in reference [19], but the relationship between the five unknown functions relevant to the peripheral TIR part needs to be derived. Since the derivation procedure is similar to that described in reference [19], however, only the results are described in this paper. First, the following three differential equations (1), (2), and (3) can be derived from the refraction of the ray on the side surface, the reflection of the ray on the TIR surface, and the refraction of the ray on the outer surface:

$$\frac{dR(\varphi)}{d\varphi} = R\frac{n\cos(\varphi+\alpha)}{1-n\sin(\varphi+\alpha)} \tag{1}$$

$$\begin{aligned}&\frac{dR}{d\varphi}[\sin\varphi - A\cos\varphi] - \frac{d\alpha}{d\varphi}l_{ab}[\sin\alpha + A\cos\alpha]\\ &+\frac{dl_{ab}}{d\varphi}[\cos\alpha - A\sin\alpha] = -R[\cos\varphi + A\ \sin\varphi],\end{aligned} \tag{2}$$

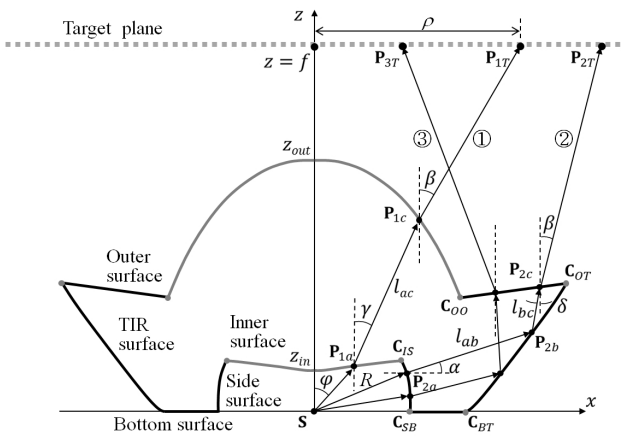

FIG. 1. Schematic diagram of a TIR LED lens composed of a central refraction part and a peripheral TIR part, and propagation of rays through both parts.

$$\frac{dR}{d\varphi}[\cos\varphi - B\sin\varphi] + \frac{d\alpha}{d\varphi} l_{ab}[\cos\alpha + B\sin\alpha] + \frac{dl_{ab}}{d\varphi}[\sin\alpha - B\cos\alpha] + \frac{dl_{bc}}{d\varphi}[\cos\delta - B\sin\delta] - \frac{d\delta}{d\varphi} l_{bc}[\sin\delta + B\cos\delta] = R[\sin\varphi + B\cos\varphi] \tag{3}$$

where A and B denote the slopes of the side surface and the outer surface, respectivley, and can be written as follows:

$$A = \tan(\pi/4 + \delta/2 - \alpha/2) \tag{4}$$

$$B = (-n\sin\delta + \sin\beta)/(n\cos\delta - \cos\beta) \tag{5}$$

The fourth differential equation is derived from the convergent illumination model and the condition for minimizing Fresnel loss, $|\beta - \delta| = |\alpha - (\pi/2 - \varphi)|$. The propagation angles δ and β may have different signs depending on the emission angle, and thus the condition for minimizing Fresnel loss can be written as the following equation (6):

$$\beta = \delta \pm (\pi/2 - \alpha - \varphi) \tag{6}$$

In addition, the emission angle φ and the radius ρ of the light reaching point must satisfy the following relationship, by the convergent illumination model:

$$\rho = \left[{\rho_{min}}^2 + ({\rho_{max}}^2 - {\rho_{min}}^2) \frac{\cos^{m+1}\varphi - \cos^{m+1}\varphi_{max}}{\cos^{m+1}\varphi_{split} - \cos^{m+1}\varphi_{max}} \right]^{1/2} \tag{7}$$

where ρ_{min} = 0 denotes the center of the target plane, and ρ_{max} denotes the maximum radius of a circular target plane. To derive this condition, the emission characteristics of the light source are assumed to have a generalized Lambertian distribution, $I(\varphi) = I_0 \cos^m\varphi$, where the superscript m is a parameter determined by the half angle $\varphi_{1/2}$ of the LED. Therefore, the actual emission characteristics of a real LED source can be considered in the design with a carefully chosen parameter m. In the meantime, the beam-spread angle θ_{spread} is defined by the maximum radius of the target plane, as follows:

$$\theta_{spread} = 2\tan^{-1}\left(\frac{\rho_{max}}{f}\right) \tag{8}$$

where f is the distance between the target plane and the point source.

Based on a simple theory of geometrical optics for ray propagation, the coordinate of a ray reaching the target plane can be written using R, the propagation angles α and δ, and the lengths l_{ab} and l_{bc}. Then the result is differentiated with respect to φ and Eq. (6) is substituted into the differentiated form, so that the fourth differential equation can be derived as follows:

$$\frac{dR}{d\varphi}[-C\cos\varphi + D\sin\varphi] - \frac{d\alpha}{d\varphi}\left[l_{ab}(C\cos\alpha + D\sin\alpha) \pm \frac{D^2}{\sin^2(\alpha + \varphi \mp \delta)} \right] + \frac{dl_{ab}}{d\varphi}[-C\sin\alpha + D\cos\alpha] + \frac{dl_{bc}}{d\varphi}[-C\cos\delta + D\sin\delta] + \frac{d\delta}{d\varphi}\left[l_{bc}(C\sin\delta + D\cos\delta) + \frac{D^2}{\sin^2(\alpha + \varphi \mp \delta)} \right] = D\left(\frac{d\rho}{d\varphi} - R\cos\varphi\right) - CR\sin\varphi \pm \frac{D^2}{\sin^2(\alpha + \varphi \mp \delta)} \tag{9}$$

$$C = \rho - (R\sin\varphi + l_{ab}\cos\alpha + l_{bc}\sin\delta) \tag{10}$$

$$D = f - (R\cos\varphi + l_{ab}\sin\alpha + l_{bc}\cos\delta) \tag{11}$$

where C and D denote x- and z-axis components of a position vector from the point $\mathbf{P}_{2c}$ on the outer surface to the point $\mathbf{P}_{2T}$ on the target plane, and $d\rho/d\varphi$ on the right side of Eq. (9) can be determined by differentiating Eq. (7) with respect to φ.

However, the five unknown functions $R(\varphi)$, $\alpha(\varphi)$, $l_{ab}(\varphi)$, $l_{bc}(\varphi)$ and $\delta(\varphi)$ relevant to the three surfaces constituting the peripheral TIR part cannot be determined by just the four differential equations; an additional constraint is required. To this end, we have introduced an equation defining the relationship between the emission angle φ and the propagation angle δ. For the convergent illumination model to be satisfied, the radius of the position where a ray reaches the target plane must be gradually reduced from ρ_{max} to 0 with increasing emission angle. Thus the propagation angle δ of the ray incident upon the outer surface must decrease monotonically from a positive maximum value to a negative minimum value with increasing emission angle φ. From this tendency, the propagation angle δ is approximated to decrease linearly with an increase in emission angle φ, as follows:

$$\delta(\varphi) = \delta_0 - k(\delta_0 + \beta_0)\left(\frac{\varphi - \varphi_{split}}{\varphi_{max} - \varphi_{split}}\right) \tag{12}$$

where δ_o and β_o denote the propagation angles when a ray whose emission angle is φ_{split} enters and emerges from the outer surface of the peripheral TIR part, and are associated with the intersection point $\mathbf{C}_{OT}$. In addition, k is a constant that determines the propagation angle when a ray whose emission angle is maximum ($\varphi = \varphi_{max}$) enters the outer surface of the peripheral TIR part. Unlike at the inner and outer

surfaces, total internal reflection is guaranteed at the TIR surface, as long as the incident angle at the surface is larger than the critical angle of the TIR surface. Thus, although an approximation such as equation (12) above is assumed, the uniform illuminance distribution and the condition for minimizing Fresnel loss will be satisfied simultaneously. As a result, the simultaneous differential equations given by Eqs. (1), (2), (3), and (9) become mathematically complete by introducing Eq. (12) additionally.

III. DESIGN PROCEDURE

To design a TIR LED lens, first the central refraction part is designed by the method proposed in reference [19]. Two intersection points with heights z_{in} and z_{out}, formed by the intersection of the inner and outer surfaces of the central refraction part with the z axis, are set as starting points, and points forming both surfaces are sequentially determined by solving the simultaneous differential equations numerically with the Runge-Kutta method [28]. This process is repeated while increasing the emission angle φ from 0 to φ_{split}. Next, surface points forming the peripheral TIR part are sequentially determined while increasing the emission angle φ from φ_{split} to φ_{max}. The illuminance distribution and luminous flux efficiency of the designed TIR LED lens are evaluated using the LightTools™ program. The flowchart for this design procedure is schematically shown in Fig. 2.

If two end points of the initially designed central refraction part can be used as starting surface points for the peripheral TIR part to be designed in sequence, the design of the peripheral TIR part will be straightforward, and also the two designed parts will be naturally combined into a complete lens. Unfortunately, this natural combination is impossible in terms of the structural characteristics of the TIR LED lens: For the two end points of the central refraction part to coincide with the starting points of the peripheral TIR, a light ray with emission angle φ_{split} should pass through the point $\mathbf{C}_{OO}$ without being reflected from the TIR surface, after entering the point $\mathbf{C}_{IS}$ on the side surface. However, if there are any rays that are not reflected from the TIR surface, then the purpose for introducing the TIR surface to reduce a deflection angle is lost. Thus the surface points of the peripheral TIR part are sequentially determined, such that the side surface starts from $\mathbf{C}_{IS}$ and is directed downward, the outer surface starts from $\mathbf{C}_{OT}$ and is directed centrally, and the TIR surface starts from $\mathbf{C}_{OT}$ and is directed downward, as in the lower inset of Fig. 2. Accordingly, the coordinate of the point $\mathbf{C}_{OT}$ and the k value of Eq. (12) should be given to design the peripheral TIR part, and the values of δ_o and β_o are determined by the coordinate of the point $\mathbf{C}_{OT}$.

If the point $\mathbf{C}_{OT}$ and the k value are not properly set, the two parts may not be completely combined with each other, as shown in Fig. 3. In Fig. 3, two points $\mathbf{C}_{OO\_C}$ and $\mathbf{C}_{OO\_P}$ respectively denote an end point forming the outer surface of the central refraction part, and an end point forming the outer surface of the peripheral TIR part. Figures 3(a) and (b) show cases where two outer surfaces intersect with each other, or the propagation of some rays having been transmitted through one part are blocked by the other part. This

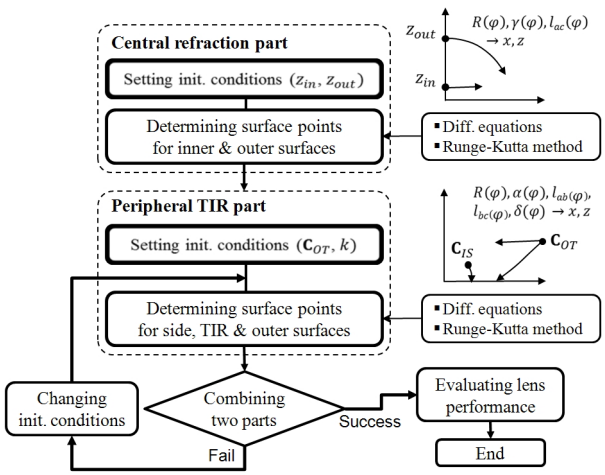

FIG. 2. The flowchart for designing a TIR LED lens with the proposed method.

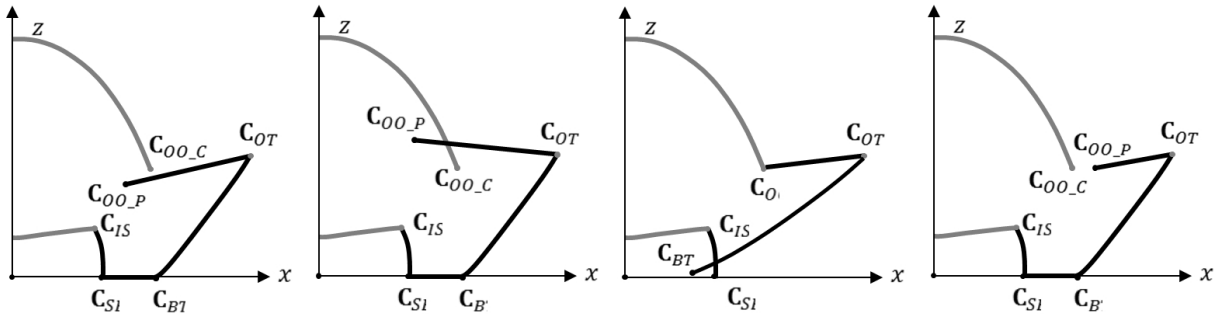

FIG. 3. Problems in combining the central refraction part with the peripheral TIR part in a TIR LED lens. (a) Partially blocking an outer surface with the other, (b) intersection of two outer surfaces, (c) intersection of the side surface with the TIR surface, and (d) wide gap between two outer surfaces.

problem can occur when $\mathbf{C}_{OT}$ is set to be too close to $\mathbf{C}_{OO}$. Meanwhile, if the k value is set too large, a ray entering the TIR surface does not satisfy the condition for total internal reflection. On the contrary, if the k value is set too small, the TIR surface and side surface may intersect, as shown in Fig. 3(c). Finally, there may be a case where two outer surfaces of the two parts are not connected to each other and do not intersect, as shown in Fig. 3(d). In this case, a complete lens can be formed by simply connecting the outer surfaces of two parts with a line. However, in the case where the source size cannot be ignored, some rays may be incident upon that line, and these rays may travel to undesired positions on the target plane, thus degrading the luminous flux efficiency and spoiling illuminance uniformity. Thus the coordinate of $\mathbf{C}_{OT}$ and the k value should be properly set, so that the outer surfaces of the central refraction and peripheral TIR parts are connected, if possible.

IV. RESULTS AND DISCUSSION

For designing TIR LED lenses with the proposed method, an LED is regarded as a point source with a generalized Lambertian emission distribution, and its half angle is assumed to be 60°. In addition, it is assumed that the center of the target plane with a circular shape is located on the z axis 1000 mm away from the point source, and that the lens is made of PMMA material with a refractive index of 1.493. The material dispersion of the lens is not considered in designing TIR LED lenses, though angular color separation is a key issue in the design of an LED lens. In the proposed method, the total deviation angle of each ray required to form uniform illumination on the target plane is equally distributed into two refractions at both the light-entering surface and the light-exiting surface of the lens, thanks to the condition for minimizing Fresnel loss, and thus material dispersion will not cause a noticeable angular color separation.

To demonstrate that the proposed method is advantageous for designing a lens having a narrow beam-spread angle, the TIR LED lenses are designed for three cases where the maximum radius ρ_{max} of the target plane is 50, 100, and 200 mm respectively. According to the definition of Eq. (8), the beam-spread angles θ_{spread} of the three TIR LED lenses are 5.7°, 11.4°, and 22.6° respectively. The split angle φ_{split} that distinguishes the central refraction part from the peripheral TIR part is commonly set to 60°. The initial parameter values used in the design of the lens are shown in Table 1, where Δx and Δz denote the x- and z-components of a vector $\mathbf{\Delta} = \mathbf{C}_{OT} - \mathbf{C}_{OO}$. The illuminance distribution and luminous flux efficiency of the designed TIR LED lens on the target plane are obtained using the LightTools™ program, where more than 5×10^5 rays are used.

In addition, three types of LED lenses are designed to compare their luminous flux efficiencies with that of the TIR LED lenses designed with the proposed method (Type IV). They are a refracting (conventional) LED lens with a single freeform surface (Type I), a refracting LED lens with double freeform surfaces (Type II), and a TIR LED lens with a single freeform surface (Type III). The light-entering surface of the Type I lens was set to be spherical during design, and then its light-exiting surface was determined as a freeform surface to satisfy the required uniform illumination on the target plane. The Type II lens was designed by the method described in reference [19], where the condition for minimizing Fresnel loss was introduced. Finally, the central and peripheral parts of the Type III lens were designed separately. The central part was designed using the same method as for the Type I lens, and the peripheral part was designed by setting its light-entering and light-exiting surfaces to be cylindrical and planar respectively.

Lens drawings and ray-tracing diagrams of the four types of LED lenses having a beam-spread angle of 5.7° are shown in Fig. 4, and comparison of their luminous flux efficiencies is shown in Fig. 5. It can be seen from Fig. 5 that the luminous flux efficiencies of the Type IV TIR LED lenses designed by the proposed method are at least 35%, 5%, and 8% higher than those of Type I, II, and III lenses respectively, and that the luminous flux efficiencies of Types II and IV lenses are higher than those of Types I and III, irrespective of beam-spread angle. Moreover, this efficiency improvement is further enhanced as the beam-spread angle becomes narrower. It is very valuable to understand how the luminous flux efficiency can be improved for either a Type IV lens designed by the proposed method or a Type II lens. From the ray-tracing diagrams shown in Fig. 4, it can be seen that the refractive characteristics of a ray at Type II and IV lenses are very different from those at Type I and III lenses. Because the condition of minimizing Fresnel loss has been

TABLE 1. Initial parameters used for designing three TIR LED lenses with the proposed method

ρ_{max} (mm)	θ_{spread} (deg.)	Central refraction part		Peripheral TIR part		
		z_{in} (mm)	z_{out} (mm)	Δx (mm)	Δz (mm)	k
50	5.7	0.90	6.00	2.45	0.00	0.478
100	11.4	0.90	6.00	2.50	0.00	0.478
200	22.6	0.90	6.00	2.97	0.00	0.478

commonly introduced for designing Type II and IV lenses, the total deviation angle of a ray required for uniform illumination is equally distributed between light-entering and light-exiting surfaces of Type II and IV lenses. Consequently, the total Fresnel loss from two surfaces can be minimized by equalizing the deviation of a ray at each surface.

For comparison, the illuminance distribution charts for Type II and IV lenses and those of the TIR LED lenses are shown on the upper and lower lines of Fig. 6 respectively, and the illuminance distribution curves are also shown in Fig. 6. Note that each chart is normalized to its own maximum illuminance, while the maximum illuminance increases as the beam-spread angle becomes narrower. It can be seen from the results of Fig. 6 that the two kinds of lenses have similar illuminance uniformities, but the bright region formed by the TIR LED lens has a clearer boundary. This superiority will be very useful for implementing a narrow uniform illumination. As a result, it can be confirmed that the simultaneous differential equations derived for the peripheral TIR part are valid.

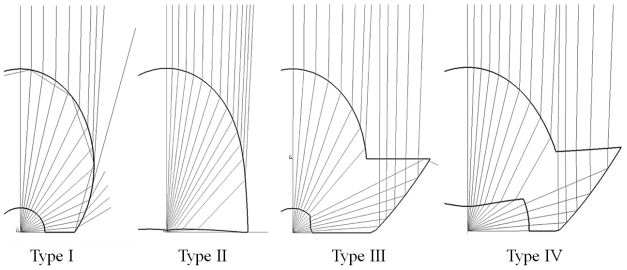

FIG. 4. Four lens drawings with ray tracing diagrams. Type I: LED lens with a single freeform surface; Type II: LED lens with double freeform surfaces; Type III: TIR LED lens with a single freeform surface; Type IV: TIR LED designed by the proposed method, in which all surfaces are freeform surfaces.

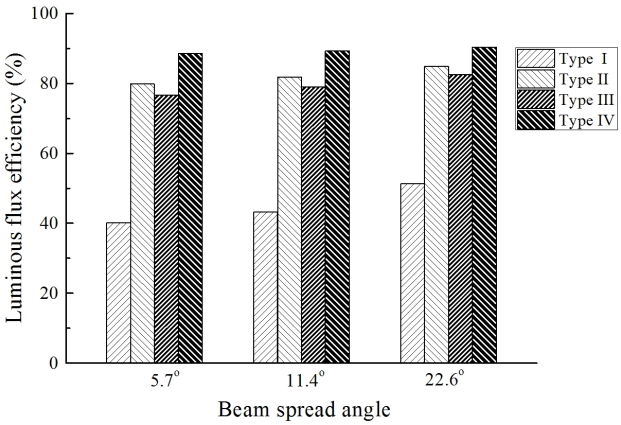

FIG. 5. Comparison of luminous flux efficiencies of four different types of lenses.

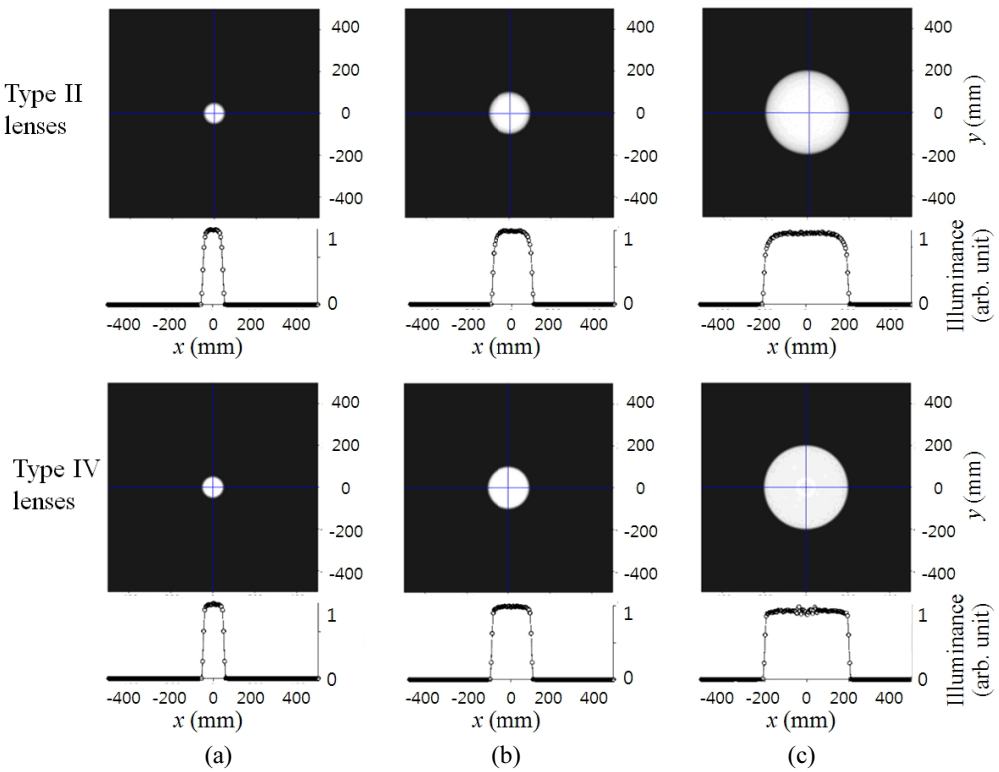

FIG. 6. Comparison of illuminance distributions of newly designed TIR LED lenses with those of conventional LED lenses with double freeform surfaces. (a) $\theta_{spread} = 5.7°$, (b) $\theta_{spread} = 11.4°$, (c) $\theta_{spread} = 22.6°$.

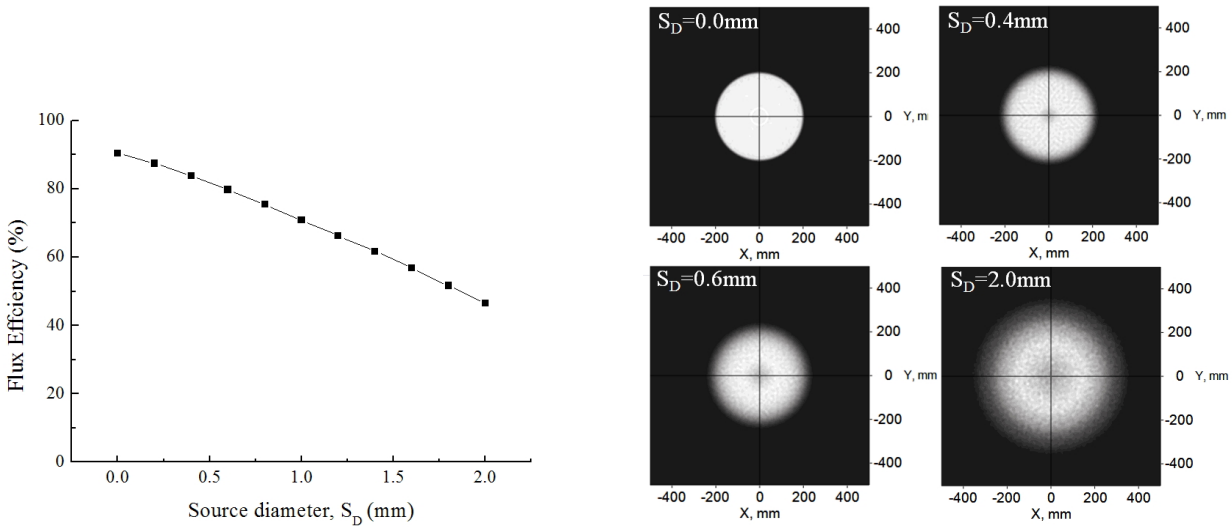

(a) (b)

FIG. 7. (a) Degradation of luminous flux efficiency with increasing source diameter, and (b) four illuminance distributions on the target plane.

As a matter of fact, the performance of the designed lens cannot but be degraded with an increase in source size, because the point-source approximation is assumed in the proposed design method. To analyze the performance degradation, the luminous flux efficiencies and the illuminance distributions on the target plane are simulated for the TIR LED lens having a beam-spread angle of 22.6°, by varying the source diameter from 0 to 2.0 mm. The variation of luminous flux efficiency with source diameter is shown in Fig. 4(a), and four illuminance distributions on the target plane are shown in Fig. 4(b), respectively. From the simulation results, it is found that the luminous flux efficiency gradually decreases with increasing source diameter and has a value of 50% for an extended source (diameter 2.0 mm), and that the illuminance distribution is seriously distorted for an extended source with diameter > 0.6 mm. Although this degradation is a common problem in differential equation methods based on the point-source approximation, it can be somewhat relieved by either raising the lens size or applying a subsequent parametric optimization method [13, 30]. Particularly, the proposed method can handle this degration in a different way: In reference [31], where the condition for minimizing the Fresnel loss was used to design a refracting LED lens with double freeform surfaces, the degradation could be relieved by modifying this condition, so a similar approach will be helpful for relieving our performance degradation, because the same condition is used. To our knowledge, this is the first method that can design all surfaces of a TIR LED lens completely composed of freeform surfaces. Consequently, it is believed that the proposed design method is valuable for realizing an LED lens with very high luminous flux efficiency and very narrow beam-spread angle.

V. CONCLUSION

To solve the problem that the luminous flux efficiency of a conventional LED lens is decreased as its beam-spread angle becomes narrower, we have proposed a novel differential equation method for designing a TIR LED lens with double freeform surfaces, in which the TIR structure is adopted to decrease deflection angles of a ray on both light-entering and light-exiting surfaces, and the condition for minimizing Fresnel loss is applied to reduce reflection loss at the surfaces. According to the proposed method, we have designed three TIR LED lenses whose beam-spread angles are 5.7°, 11.4°, and 22.6° respectively, and evaluated their luminous flux efficiencies and illuminance destributions. It can be seen from the results that the luminous flux efficiencies of the TIR LED lenses can be increased by at least 35% and 5%, compared to those for conventional LED lenses with a single freeform surface and double freeform surfaces respectively. In addition, it is confirmed that the improvement in luminous flux efficiency is more effective as the beam-spread angle becomes narrower. However, the performance of the lens designed by the proposed method is degraded with increasing size of the LED source, and thus a study to enhance lens performance for an extended source via modifying the condition for minimizing the Fresnel loss remains a topic for further investigation.

ACKNOWLEDGEMENT

This work was supported by INHA UNIVERSITY Research Grant (51930-1).

REFERENCES

1. J. Jiang, S. To, W. B. Lee, and B. Cheung, "Optical design of a freeform TIR lens for LED streetlight," Optik **121**, 1761-1765 (2010).
2. N. Shatz, J. Bortz, J. Matthews, and P. Kim, "Advanced optics for LED flashlights," Proc. SPIE **7059**, 1-12 (2008).
3. B. W. Kim, J. G. Kim, W. S. Ohm, and S. I. Kang, "Eliminating hotspots in a multi-chip LED array direct backlight system with optimal patterned reflectors for uniform illuminance and minimal system thickness," Opt. Express **18**, 8595-8604 (2010).
4. H. C. Chen, J. Y. Lin, and H. Y. Chiu, "Rectangular illumination using a secondary optics with cylindrical lens for LED street light," Opt. Express **21**, 3201-3212 (2013).
5. B. J. Kim, D. C. Kim, B. H. O, S. G. Park, B. H. Kim, and S. G. Lee, "Optimal Design of Secondary Optics for Narrowing the Beam Angle of an LED Lamp with a Large-Area COB-type LED Package," Korean J. Opt. Photon. **25**, 78-84 (2014).
6. J. h. Wang, Y. C. Liang, and M. Xu, "Design of a See-Through Head-Mounted Display with a Freeform Surface," J. Opt. Soc. Korea **19**, 614-618 (2015).
7. Q. F. Zhang, J. Gao, and X. Chen, "Influence of optical aspheric parameters on obtaining uniform rectangular illumination," Optik **125**, 2577-258 (2014).
8. F. R. Fournier, W. J. Cassarly, and J. P. Rolland, "Fast freeform reflector generation using source-target maps," Opt. Express **18**, 5295-5304 (2010).
9. Y. Luo, Z. X. Feng, Y. J. Han, and H. T. Li, "Design of compact and smooth free-form optical system with uniform illuminance for LED source," Opt. Express **18**, 9055-9063 (2010).
10. B. C. Kim, D. W. Kim, and G. H. Kim, "Free-Form Surface Reconstruction Method from Second-Derivative Data," Korean J. Opt. Photon. **25**, 273-278 (2014).
11. G. Z. Wang, L. L. Wang, L. Li, D. D. Wang, and Y. J. Zhang, "Secondary optical lens designed in the method of source-target mapping," App. Opt. **50**, 4031-4036 (2011).
12. X. J. Hu and K. Y. Qian, "Optimal design of optical system for LED road lighting with high illuminance and luminance uniformity," App. Opt. **52**, 5888-5893 (2013).
13. P. Liu, R. M. Wu, Z. R. Zheng, H. F. Li, and X. Liu, "Optimized design of LED freeform lens for uniform circular illumination," J. Zhejiang U. SCI. C (Comput. & Electron.) **13**, 929-936 (2012).
14. E. G. Chen, P. Liu, and F. H. Yu, "Synchronized parameter optimization of the double freeform lenses illumination system used for the CF-LCoS pico-projectors," Opt. & Las. Technol. **44**, 2080-2087 (2012).
15. E. Vidal, D. Otaduy, F. Gonzalez, J. M. Saiz, F. Moreno, and Y. Wang, "Design and optimization of a collimating optical system for high divergence LED light sources," Proc. SPIE **7428**, 1-10 (2009)
16. D. Grabovickic, P. Benitez, and J. C. Minano, "Aspheric V-groove reflector design with the SMS method in two dimensions," Opt. Express **18**, 2515-2521 (2010).
17. W. Lin, P. Benitez, J. C. Minano, J. M. Infante, and G. Biot, "SMS-based optimization strategy for ultracompact SWIR telephoto lens design," Opt. Express **20**, 9726-9735 (2012).
18. J. C. Minano, P. B. Tez, and A. Santamaria, "Free-Form Optics for Illumination," Opt. Rev. **16**, 99-102 (2009).
19. M. A. Moiseev, S.V. Kravchenko, L. L. Doskolovich, and N. L. Kazanskiy, "Design of LED optics with two aspherical surfaces and the highest efficiency," Proc. SPIE **8550**, 1-6 (2012).
20. R. Hu, Z. Q. Gan, X. B. Luo, H. Zheng, and S. Liu, "Design of double freeform-surface lens for LED uniform illumination with minimum Fresnel losses," Optik **124**, 3895- 3897 (2013).
21. H. Wu, X. M. Zhang, and P. Ge, "Double freeform surfaces lens design for LED uniform illumination with high distance-height ratio," Opt. & Las. Technol. **73**, 166-172 (2015).
22. S. Hu, K. Du, T. Mei, L. Wan, and N. Zhu, "Ultra-compact LED lens with double freeform surfaces for uniform illumination," Opt. Express **23**, 20350-20355 (2015).
23. A. B¨auerle, A. Bruneton, R. Wester, J. Stollenwerk, and P. Loosen, "Algorithm for irradiance tailoring using multiple freeform optical surfaces," Opt. Express **20**, 14477-14485 (2012).
24. Y. Zhang, R. M. Wu, P. Liu, Z. R. Zheng, H. F. Li, and X. Liu, "Double freeform surfaces design for laser beam shaping with Monge–Ampere equation method," Opt. Commun. **331**, 297-305 (2014).
25. V. I. Oliker, "Mathematical aspects of design of beam shaping surfaces in geometrical optics," in *Trends in Nonlinear Analysis*, M. Kirkilionis, S. Krömker, R. Rannacher, F. Tomi, eds. (Springer, 2003).
26. H. B. Cheng, C. Y. Xu, X. L. Jing, and H. Y. Tam, "Design of compact LED free-form optical system for aeronautical illumination," App. Opt. **54**, 7632-7639 (2015).
27. H. Xiang, Z. Z. Rong, L. Xu, and G. P. Fu, "Freeform surface lens design for uniform illumination," Pure Appl. Opt. **10**, 1-6 (2008).
28. J. Chistiansen, "Numerical Solution of Ordinary Simultaneous Differential Equations of the 1st Order Using a Method for Automatic Step Change," Numer. Math. **14**, 317-324 (1970).
29. X. X. Luo, H. Liu, Z. W. Lu, and Y. Wang, "Automated optimization of an aspheric light-emitting diode lens for uniform illumination," App. Opt. **50**, 3412-3418 (2011).
30. M. A. Moiseeva, L. L. Doskolovicha, K. V. Borisovab, and E. V. Byzovb, "Fast and robust technique for design of axisymmetric TIR optics in case of an extended light source," J. Mod. Opt. **60**, 1100-1106 (2013)
31. M. A. Moiseev, E. V. Byzov, S. V. Kravchenko, and L. L. Doskolovich, "Design of LED refractive optics with predetermined balance of ray deflection angles between inner and outer surfaces," Opt. Exp. **23**, A1140-A1148 (2015).